Link to published version (if available):

Link to publication record in Explore Bristol Research
PDF-document

University of Bristol - Explore Bristol Research

Case Study

Analysis of Structural Health Monitoring Data from Hammersmith Flyover

G. T. Webb[1]; P. J. Vardanega, Ph.D., M.ASCE[2]; P. R. A. Fidler[3]; and C. R. Middleton, Ph.D., C.Eng.[4]

Abstract: There has recently been considerable research published on the applicability of monitoring systems for improving civil infrastructure management decisions. Less research has been published on the challenges in interpreting the collected data to provide useful information for engineering decision makers. This paper describes some installed monitoring systems on the Hammersmith Flyover, a major bridge located in central London (United Kingdom). The original goals of the deployments were to evaluate the performance of systems for monitoring prestressing tendon wire breaks and to assess the performance of the bearings supporting the bridge piers because visual inspections had indicated evidence of deterioration in both. This paper aims to show that value can be derived from detailed analysis of measurements from a number of different sensors, including acoustic emission monitors, strain, temperature and displacement gauges. Two structural monitoring systems are described, a wired system installed by a commercial contractor on behalf of the client and a research wireless deployment installed by the University of Cambridge. Careful interpretation of the displacement and temperature gauge data enabled bearings that were not functioning as designed to be identified. The acoustic emission monitoring indicated locations at which rapid deterioration was likely to be occurring; however, it was not possible to verify these results using any of the other sensors installed and hence the only method for confirming these results was by visual inspection. Recommendations for future bridge monitoring projects are made in light of the lessons learned from this monitoring case study. **DOI: [10.1061/(ASCE)BE.1943-5592.0000587](#).** *This work is made available under the terms of the Creative Commons Attribution 4.0 International license, http://creativecommons.org/licenses/by/4.0/.*

Introduction

Literature Review

Many studies have been published recently that describe the deployment of extensive structural health monitoring (SHM) systems in which both wireless (e.g., Lynch et al. 2006; Hoult et al. 2008a, b, 2010b; Kurata et al. 2013) and wired (e.g., Wong 2004; Shoukry et al. 2009; Dwairi et al. 2010) data communications systems have been employed. The state of the art (of wireless sensor deployments) has been outlined in several review papers (e.g., Lynch and Loh 2006; Lynch 2007), along with the various advantages and disadvantages of using wireless systems as compared with traditional wired sensing equipment. More broadly, the papers of Maser (1988) and Farrar and Worden (2007) give general advice on the challenges of using SHM to obtain useful information for engineering decision making.

[1]Doctoral Student, Dept. of Engineering, Univ. of Cambridge, Cambridge CB2 1PZ, U.K. E-mail: graham.webb@cantab.net

[2]Lecturer in Civil Engineering, Dept. of Civil Engineering, Univ. of Bristol, Bristol BS8 1TR, U.K.; formerly, Research Associate, Dept. of Engineering, Univ. of Cambridge, Cambridge CB2 1PZ, U.K. (corresponding author). E-mail: pv13522@bristol.ac.uk

[3]Computer Associate, Dept. of Engineering, Univ. of Cambridge, Cambridge CB2 1PZ, U.K. E-mail: praf1@cam.ac.uk

[4]Laing O'Rourke Professor of Construction Engineering, Dept. of Engineering, Univ. of Cambridge, Cambridge CB2 1PZ, U.K. E-mail: crm11@cam.ac.uk

More advanced analyses using data from SHM systems have also been carried out, in some cases to determine the optimum locations of sensors for new deployments (e.g., Kripakaran and Smith 2009; Laory et al. 2012) and in others, to falsify model variants using different combinations of material parameters and boundary conditions that influence the behavior of the structure (e.g., Goulet et al. 2010).

Catbas et al. (2007) discuss the limitations of large SHM systems and caution against an overreliance on finite-element modeling to interpret SHM data. SHM monitoring efforts studying the effects of temperature (e.g., Chang and Im 2000) and studies attempting to match finite-element analyses to the measured data during bridge load tests (e.g., Hedegaard et al. 2013) have also been carried out.

Often, an overall goal of SHM systems is to detect damage or deterioration to a structure. Minardo et al. (2012) describe an example in which this was achieved. There are, however, surprisingly few such examples in which data from monitoring systems are interpreted to provide useful information about the health of the structure being monitored.

The current paper has two parts. First, the challenges of obtaining data from two independent SHM systems installed on the Hammersmith Flyover in London (United Kingdom) are presented. More specific details of some aspects of these deployments are described in Hoult et al. (2010a) and Watson (2010). The second part of the paper discusses the results of subsequent postprocessing and interpretation of the gathered monitoring data by the Cambridge University team, to investigate the value that can be gleaned.

Hammersmith Flyover

This paper discusses the collection and interpretation of data from two independent SHM systems installed on the Hammersmith Flyover in London, United Kingdom (Fig. 1). The original design of

Fig. 1. The Hammersmith Flyover (image courtesy of Dr. Peter Bennett, taken August 26, 2009)

Fig. 2. Corrosion of prestressing tendons (image by authors, taken May 14, 2012)

Fig. 3. Roller bearings supporting a bridge pier (image courtesy of Dr. Peter Bennett, taken September 22, 2009)

this critical piece of transport infrastructure is detailed in the papers of Rawlinson and Stott (1962) and Wroth (1962).

Constructed in the early 1960s, the Hammersmith Flyover carries four lanes of a strategic road transport artery, the A4 trunk road, into London from the west. It is a 622-m-long, 16-span, partially bonded, posttensioned, segmental, cellular concrete bridge supported on RC piers. The flyover has roller bearings at the base of each pier, is restrained against longitudinal movement at each abutment, and has a single expansion joint toward the center of the bridge.

In recent years, concerns have arisen about the condition and live load capacity of the flyover, primarily as a result of observed corrosion of the prestressing tendons, which has been accelerated by the application of deicing salts during winter and the failure of the waterproofing system. Although corrosion had been a concern for many years, recent intrusive inspections found it to be far more severe than had been expected (Fig. 2). A second concern was the performance of the roller bearings (photographed in Fig. 3) and

whether deterioration was resulting in a restraint against expansion as symbolized in the schematic in Fig. 4. Thermal movement is accommodated by roller bearings at the base of each pier. Restraint in the bearings due to corrosion would induce additional bending moments in the piers and deck, potentially causing an opening of the joints between segments and exacerbating the stress levels in the corroded prestressing tendons.

The Engineering and Physical Sciences Research Council (EPSRC) research project *Smart Infrastructure: Wireless sensor network system for condition assessment and monitoring of infrastructure* (2006–2009) aimed to showcase the application of wireless sensor networks (WSNs) across multiple infrastructure types (e.g., bridges, tunnels, and water pipelines). One of the aims of the project was to install a WSN in parallel with a wired monitoring solution installed independently by a contractor, thus allowing the costs, reliability, and performance of both the systems to be compared.
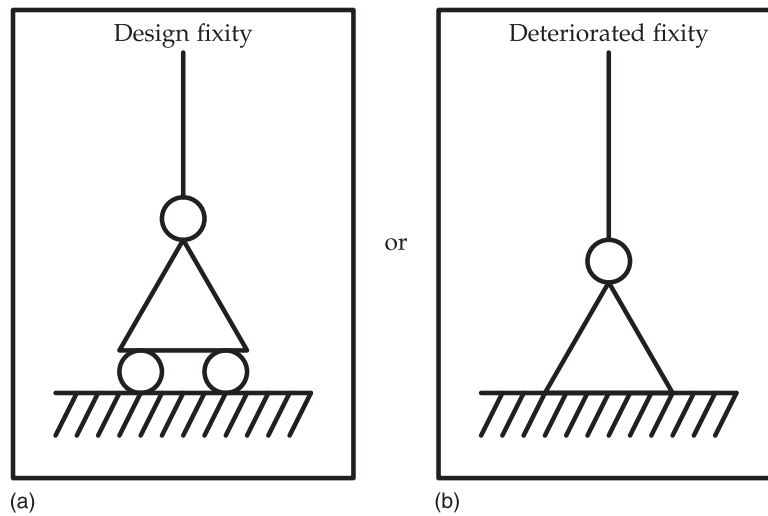
Fig. 4. (a) Symbolic representation of fixity of bridge roller bearing as designed and (b) possible actual operational fixity in the deteriorated state

Installed Monitoring Systems

This section describes the deployment of the monitoring systems installed on the Hammersmith Flyover. A wireless system, hereafter referred to as the Research System, was deployed as part of the research work by Cambridge University. A separate, independent wired system, hereafter referred to as the Commercial System, was installed by Physical Acoustics Ltd. (Watson 2010) for the bridge owners, Transport for London (TfL). Fig. 5 shows representative locations of the installed monitoring devices from both systems (excluding the acoustic monitoring system).

Research System (University of Cambridge)

The Research System was installed during August and September 2009. Details of the installed equipment are explained briefly in Hoult et al. (2010a). The system was designed to measure strain and inclination at four of the piers, and the longitudinal displacement of their bearings. In addition, inclinations of retaining walls in the Hammersmith underground train station were measured, to monitor movements that could have resulted from some nearby construction works. The train station retaining wall data are not considered in this paper.

It was decided not to attempt to install wireless acoustic emission (AE) sensors to detect breaks in the prestressing tendons as part of the Research System, mainly because access to the confined space inside the bridge deck box made long-term maintenance of the sensors difficult. In addition, battery-powered wireless AE sensors are not ideal for detecting wire breaks, which can occur at any time, because the need to monitor continuously results in a large drain on power and hence battery life is reduced significantly. Wireless sensors are better suited for measuring parameters that change slowly and can therefore be sampled at a low rate (e.g., temperature, inclination, or displacement).

Two linear potentiometric displacement transducers (LPDTs) were installed in each of the four bearing pits to detect horizontal motion of the piers on their bearings. In addition, six inclinometers were installed on the sides of the piers themselves. Similar LPDTs had already been used by the researchers on previous sites, but with low-resolution 10-bit analog to digital converters (ADCs) to measure displacement. Late in the project, it was decided to use LPDTs

to also measure strain in the piers, requiring a redesign of the circuit board to accommodate a 16-bit ADC for greater resolution. Each of the inclinometers was paired with an LPDT sensor to measure strain and they were installed together in a single box fixed to the exterior concrete walls of the piers (Fig. 5). Each measurement location also included a relative humidity and temperature sensor. In addition, each pier required one relay module (mote) to facilitate network connectivity. This resulted in 15 wireless nodes per pier: a total of 60 nodes on the flyover. Combined with the 44 nodes installed at Hammersmith Station, the entire network consisted of 104 nodes, meeting a demonstration goal of having more than 100 wireless nodes in the network.

Commercial System (Physical Acoustics)

The Commercial System, installed between April and July 2010, comprised around 300 AE sensors for detecting wire breaks in the prestressing tendons, and a number of other sensors, including inclinometers and strain gauges on the interior of the piers, robotic survey total stations, temperature sensors, and displacement transducers (Watson 2010) (photos of some of the installed devices from both the wireless and wired deployments are shown in Fig. 6). The Commercial System sensors were wired to a data logger housed in a cabinet at the eastern abutment of the flyover. Although the authors had no involvement in the design, installation, or operation of the Commercial System, the data obtained by this system were made available by the client (TfL) for analysis.

The acoustic signature of each possible wire break detected by the commercial system was interpreted by Physical Acoustics Ltd. using a proprietary method. This method is claimed to be able to distinguish between wire breaks and other similar-sounding events. The results reported to the client indicated the time at which each *confirmed* wire break occurred and the location to the nearest 500 mm. The location accuracy was verified by a blind test during commissioning (Watson 2010).

An analysis of some of the commercial sensor data is presented later in this paper. The only data from the Research System used in the analysis presented here are those obtained from the displacement gauges at the base of the piers, which enabled comparison between the data obtained from the commercial wired and research wireless SHM systems. Fig. 7 shows that the commercial and research
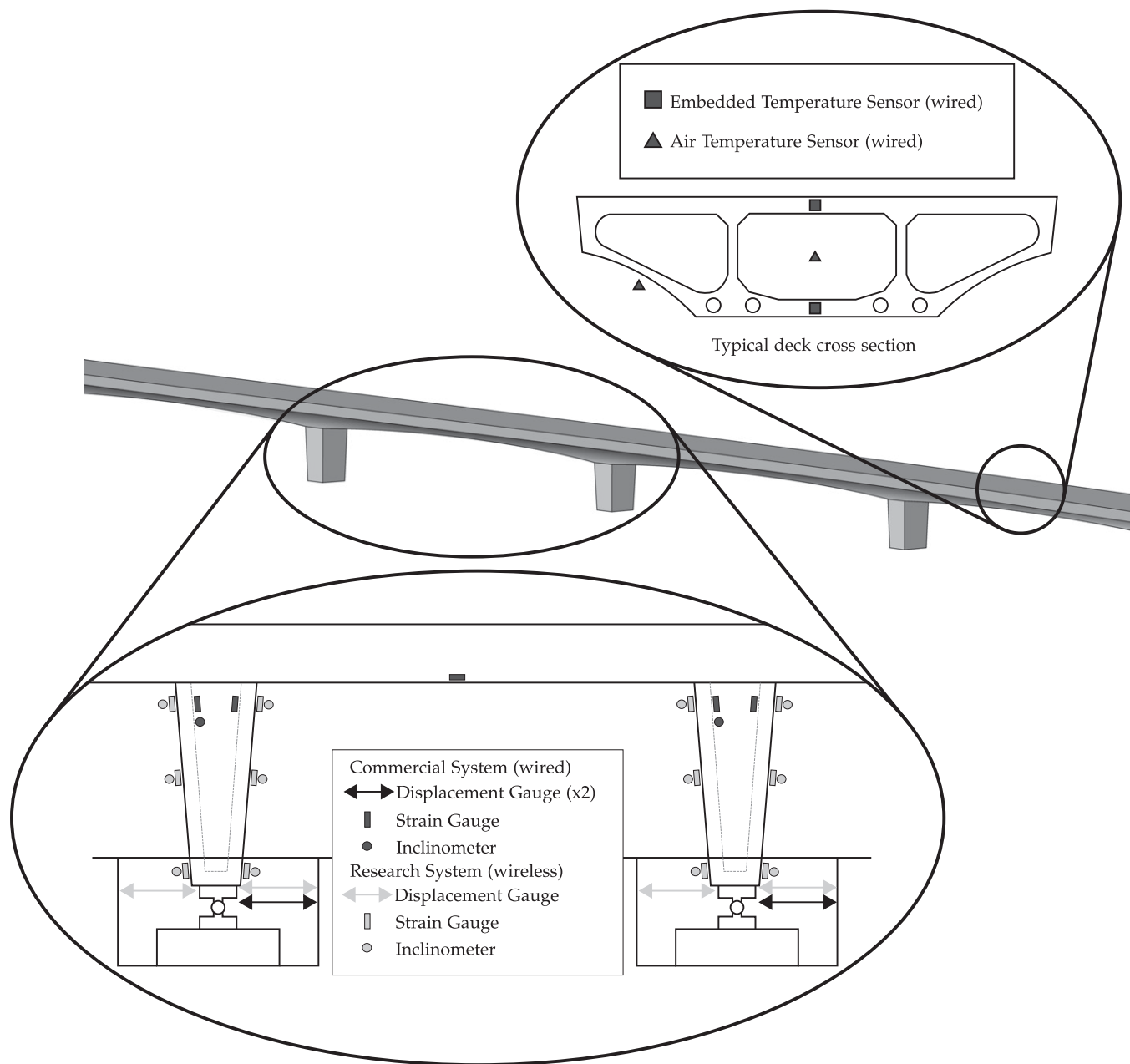
Fig. 5. Representative locations of metrology devices on Hammersmith Flyover

systems both provided very similar readings for displacement at the base of the piers.

Challenges Encountered during the Monitoring (Research System)

In reporting on some other aspects of the Hammersmith WSN deployment, Hada et al. (2011) describe how data from WSNs can be lost because of the effects of passing trains on radio signal propagation in railway tunnels. This section discusses other challenges that were encountered during the installation and operation of the sensors on the Hammersmith Flyover.

LPDT Displacement Sensors
A hardware circuit fault was identified in the LPDT sensor boards after installation. The actual board layout design used did not match the intended schematic. These boards had been designed very shortly before the field deployment and, as a result of time constraints, were installed without adequate calibration and testing, which would have revealed the fault. Eventually new circuit boards were designed and manufactured by the lead author and were installed in March 2012, replacing the faulty boards.

Data Logger
The Research System currently has no provision for storing data locally on the sensor nodes. When the sensor nodes take a reading from their sensor, it is transmitted immediately, either directly to the wireless data logger or via other nodes. Each sensor node/mote acts as a relay router so data are able to hop from node to node until they reach the data logger, where they are recorded before being sent via an internet-connected 3G modem to a database server. The data
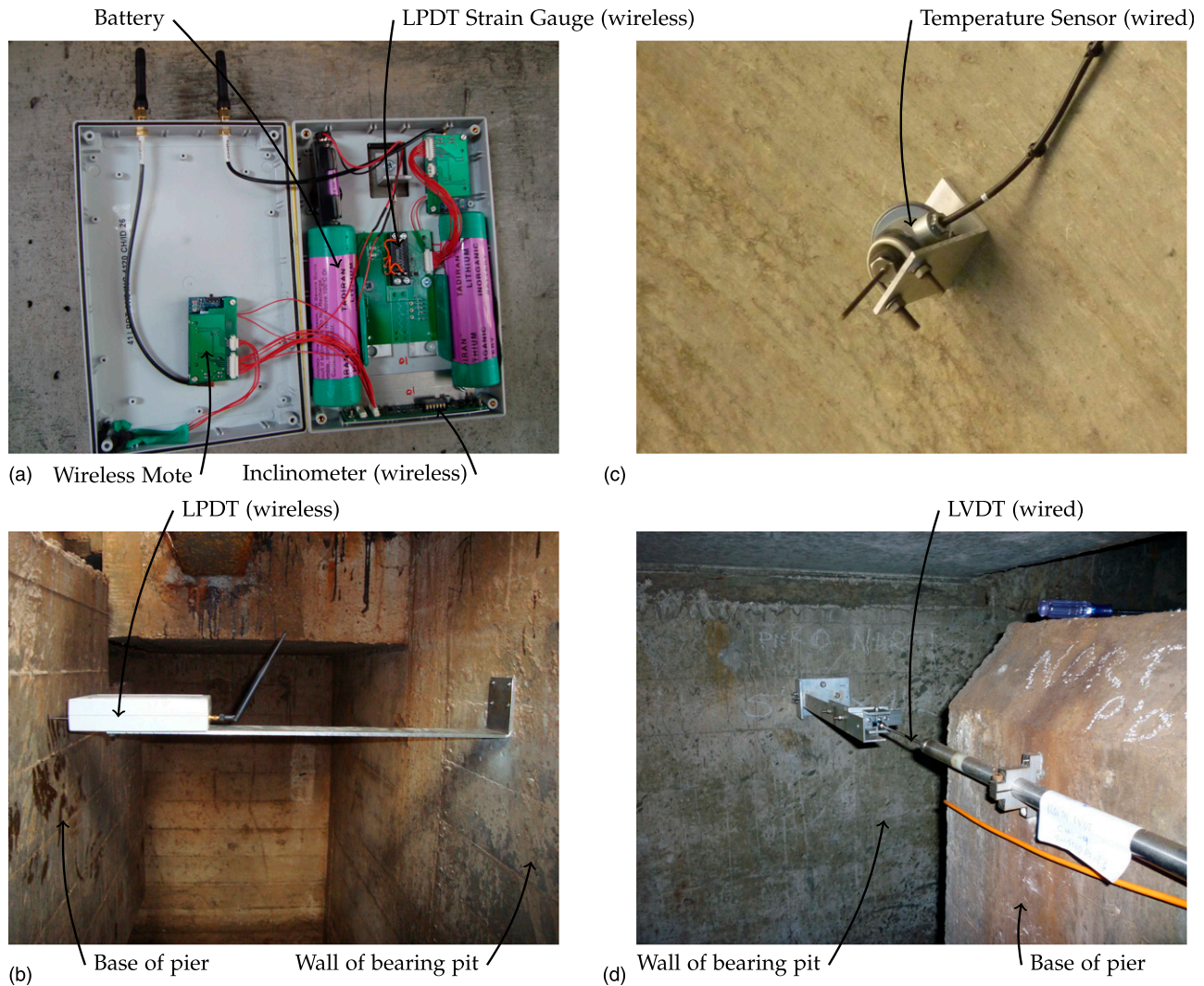
Fig. 6. Some sensors used in the monitoring study; photos taken on (a) August 26, 2009 (image courtesy of Dr. Peter Bennett); (b) September 22, 2009 (image courtesy of Dr. Peter Bennett); (c) February 8, 2011 (image by authors); (d) February 8, 2011 (LVDT = linear variable differential transformer; image by authors)
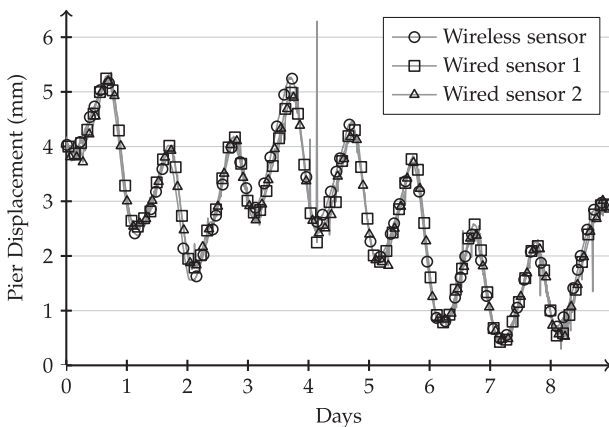

Fig. 7. Comparison of data from commercial wired and research wireless monitoring systems (start date March 22, 2012)

logger for the system is positioned at the end of a train platform at Hammersmith Station. There is no direct line of sight between the sensors on the flyover and the data logger; therefore, for data from a particular node to be recorded successfully, there must be a path from node to node all the way to the data logger, and the data logger must be functioning. Since the original installation in September 2009, the data logger has proved to be somewhat unreliable, having failed twice because of issues with the embedded operating system and the flash-based file-system, at least once because of a power failure, and once because of a loose connection between the wireless receiver and a serial-to-USB adapter.

Flooding

During remedial strengthening work to the flyover (undertaken by TfL's contractor between January and May 2012), water from the water-jetting operations on the deck (to remove the old central reservation) found its way through the structure into the bearing pits. When the packaging for the LPDT and inclinometer sensors was designed, it was not anticipated that the bearing pits would flood; the pits had soakaway drainage and the flyover itself prevented rain falling directly onto the area surrounding the pits. The result was
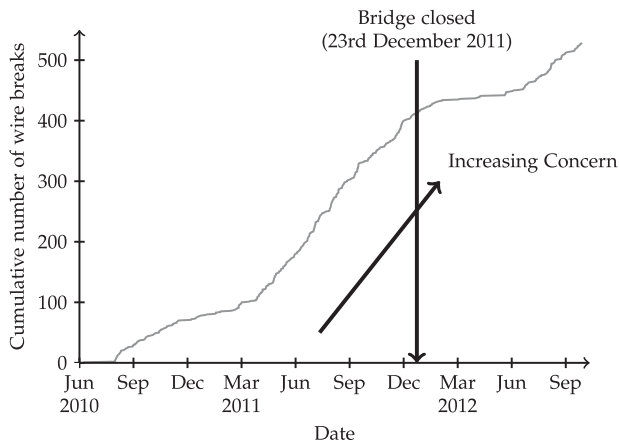
Fig. 8. Cumulative wire breaks in all spans (2010–2012)

damage to several inclinometer sensors. (The nonfunctional LPDT sensors with faulty circuit boards had by this stage been removed to be replaced by new sensor boards.)

Interpretation of Monitoring Data: Loss of Prestress

The commercial AE system was installed with the aim of detecting wire breaks in the prestressing tendons in the deck box section. Fig. 8 shows a cumulative plot of the number of wire breaks detected throughout the whole bridge by the AE system over approximately 2 years. Investigations following from the results of the AE monitoring led to the closure of the bridge for emergency repairs on December 23, 2011. It might be expected that losses of prestressing force would result in a change in longitudinal strain in the bridge deck. The installed monitoring systems included a limited number of gauges at critical sections measuring longitudinal strain in the deck, and a study was undertaken by the University of Cambridge research team to determine what magnitude of strain is caused by different levels of prestress loss, although it was anticipated that these strains would be very small.

Estimated Loss of Prestress: Analysis

To relate the AE monitoring results to structural performance, one must consider how wire breaks affect the structure. Because of uncertainty about how much rebonding of the prestressing tendons actually occurs once a break results, TfL assumed that there was no rebonding of the individual broken wires between the grouted midspan sections of the tendon runs, and breaks were assumed to be cumulative (K. Duguid, personal communication, 2013). The simple hypothetical analysis that follows, however, does assume some rebonding, with the aim of providing quantitative estimates of the deck strains that follow wire breaks.

When a single prestressing wire ruptures, the structural effect is complex because it is assumed that some of the force will be transferred into neighboring wires because of friction. This effect can be explored by considering a simple hypothetical case of a single prestressed concrete beam of length l, with gross concrete cross-sectional area A_c, and prestressing steel wires of total cross-sectional area A_s (Fig. 9). In the analysis that follows, compression will be taken as positive. Bending moments will be neglected initially, with only the axial forces being considered. It will also be assumed that the prestressing tendons are unbonded and that there is therefore no friction force between the wires and the concrete. The tendons in the
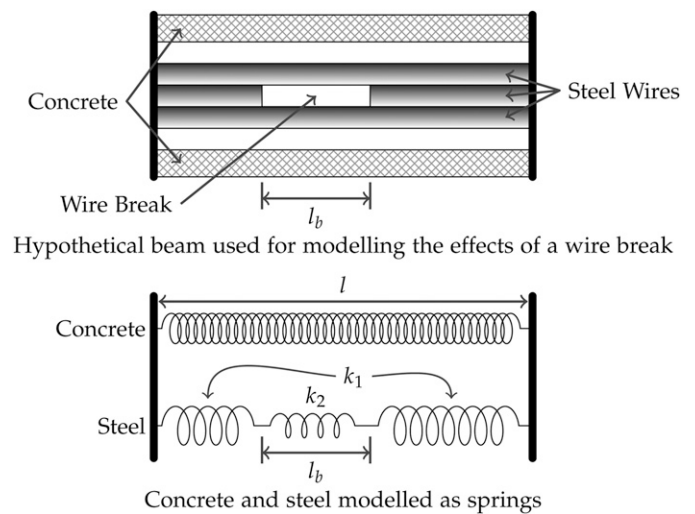

Hypothetical beam used for modelling the effects of a wire break

Concrete and steel modelled as springs

Fig. 9. Modeling effects due to loss of prestress

Hammersmith Flyover were enclosed by a grout surround after stressing; however, this was to protect against corrosion rather than to provide any structural bond and did not have a structural shear connection to the webs of the box beam. Visual and intrusive inspections showed the grout to be of variable quality, and any bond that did exist could not be relied on. If the initial total prestressing force in all the wires, F_i, is known, then the initial concrete stress (compressive), σ_{ci}, and steel stress (tensile), σ_{si}, can be determined. These will both be constant over the length of the hypothetical beam. At a wire break, the two ends of the broken wire will attempt to shorten. This shortening will be resisted by friction between the wire and its adjacent wires and hence there will be a certain distance from the break beyond which no slip occurs and the tendon is unaffected. An effective break length, l_b, can be defined over which the steel cross-sectional area is taken to have been reduced by the area of the broken wire, ΔA_s. Outside this length, the cross-sectional area of the steel remains unaffected (see Fig. 9).

In the instant immediately after the break, the overall force carried by all the steel wires, $F_s = -F_i$, will remain unchanged. There will therefore be a stress change in the remaining unbroken steel wires over the effective break length, where the cross-sectional area of steel is reduced

$$\Delta\sigma_s = \frac{F_s}{A_s - \Delta A_s} - \frac{F_s}{A_s} \qquad (1)$$

This stress change will cause a strain change in the steel wires over the effective break length and therefore the overall length of the steel tendon will increase

$$\Delta l = \frac{\Delta\sigma_s}{E_s} l_b \qquad (2)$$

This means the concrete must also change length by the same amount, and hence the compressive force in the concrete will be reduced to

$$F_c = F_i + \left(\frac{\Delta l}{l} E_c A_c\right) \qquad (3)$$

This would mean that the compressive force in the concrete and the tensile force in the steel would no longer be in equilibrium. The overall length of the beam must then be allowed to vary until equilibrium is restored.

Because the steel does not now have a constant cross section along its length, a new effective stiffness must be calculated. Both the steel and the concrete can be modeled as springs as shown in Fig. 9. The steel can be split into different segments, each with its own cross-sectional area and axial stiffness, depending on the number of wires present and the length of the segment. Outside the effective break length, where the full cross-sectional area of the steel wires is present, the stiffness is denoted as k_1. Within the effective break length, there is a reduced area of steel and hence a different axial stiffness, denoted as k_2. An overall effective axial stiffness of the steel, $k_{s,\text{eff}}$, can then be calculated using the equation for springs in series

$$\frac{1}{k_{s,\text{eff}}} = \frac{1}{k_1} + \frac{1}{k_2} \tag{4a}$$

$$\frac{1}{k_{s,\text{eff}}} = \frac{1}{\left(\dfrac{A_s E_s}{l - l_b}\right)} + \frac{1}{\left[\dfrac{(A_s - \Delta A_s)E_s}{l_b}\right]} \tag{4b}$$

The change in length, x, required to restore equilibrium and the new forces in the steel, $F_{s,\text{new}}$ and concrete, $F_{c,\text{new}}$, can then be found from the following equations:

$$F_{s,\text{new}} = F_s + x k_{s,\text{eff}} \tag{5}$$

$$F_{c,\text{new}} = F_c + x \frac{A_c E_c}{l} \tag{6}$$

$$F_{s,\text{new}} + F_{c,\text{new}} = 0 \tag{7}$$

The strain change in the concrete, $\Delta\varepsilon_c$, can then be calculated from the total change in length

$$\Delta\varepsilon_c = \frac{\Delta l + x}{l} \tag{8}$$

Each span of the Hammersmith Flyover is approximately 40 m in length and originally contained four tendons of 16, 19-wire strands (giving a total of $4 \times 16 \times 19 = 1,216$ wires midspan) that lapped over alternate piers increasing the number of wires in the midspan region (1,216) to 1,824 in the critical regions over the piers. Each wire has a cross-sectional area of 28 mm². The tendons were stressed to give a total force after losses of approximately 30 MN (Rawlinson and Stott 1962). The analysis presented earlier can be used to predict the loss of prestressing force and the resulting concrete strain caused by increasing numbers of wire breaks (by increasing ΔA_s). Although the cross-sectional area of the concrete sections varies along the length of the bridge, an averaged value of 6.46 m² has been used in this analysis. Fig. 10 shows how the predicted longitudinal concrete strain increases with the number of wire breaks for a range of different effective break lengths, l_b: the resulting strains are very small. If approximately 20% of the total number of wires at any cross section snapped and became ineffective over a 10-m effective break length, the concrete strain induced would be less than $10\,\mu\varepsilon$. Also, the overall prestressing force changes very little when such an event occurs, resulting in the steel stress increasing over the distance in which the broken wire is ineffective. Eventually, with sufficient wire breaks, this situation could become hazardous because the increasing stress in the remaining unbroken wires would result in rupture, leading to a sudden loss of prestress and collapse of the structure. Because the predicted strains are so small, it was decided not to extend the analysis to consider the effects of bending moments caused by the eccentricity of the prestressing tendon.
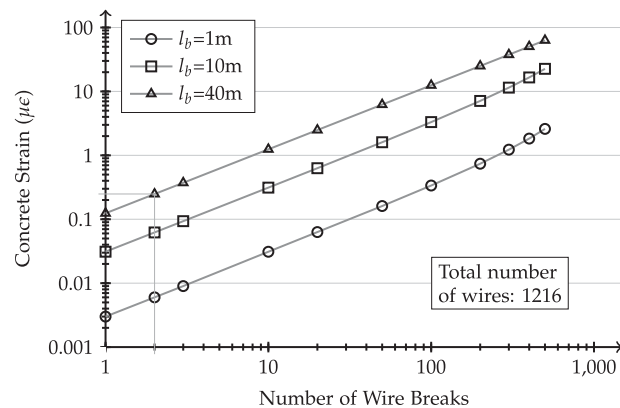

Fig. 10. Calculation of concrete strain variation versus number of wire breaks (assuming unbonded tendons)

The plot in Fig. 10 assumes that all wire breaks occur in different wires and at the same location along the beam; however, this is unlikely to be manifested in practice in the field. It is thus necessary to consider how subsequent breaks affect a tendon that already contains wire breaks at other locations. When a wire break occurs, the tension in that individual wire is assumed to reduce to zero over the effective break length, meaning it cannot break again within that region. If another wire break is detected in the same area of the tendon, it must therefore be a different wire. If, instead, the next wire break occurs farther away, it could be in any wire, including the already broken wire, because a wire break is assumed to not affect the wire outside the effective break length. In this case, the effect on the whole tendon will be the same as a single wire break with an increased effective break length.

It is claimed that the commercial AE sensor monitoring system can locate each detected wire break (to within 500 mm) so it is possible to estimate the expected change in longitudinal strain in the concrete. During the commissioning of the AE monitoring system, a small number of wires in the prestressing tendons were cut, to determine whether the system could correctly locate suspected wire breaks. The two ends of each cut wire were observed to shorten by approximately 5–10 mm. This can be used to estimate a value to use for the effective break length, l_b. The shortening, y, is caused by the reduction in stress and hence strain, which occurs throughout the effective break length. Because the initial stress in the steel wires is known, the length over which the stress reduction occurs can be estimated

$$l_b = \frac{y E_s}{\Delta\sigma_w} = \frac{10\ \text{mm} \times 200\ \text{GPa}}{872\ \text{MPa}} \approx 2\ \text{m} \tag{9}$$

Wire break location data obtained from the AE system were then used to count the number of breaks in each 2-m-long section of the bridge. The results gave an average of two breaks per 2 m over the full length of the bridge. Using the reasoning from the previous paragraph, the longitudinal strain change in each span can therefore be predicted from Fig. 10, with an assumed number of breaks of two and an increased break length of 40 m (i.e., one span). This would result in a change in concrete strain of the order of $0.2\,\mu\varepsilon$.

The Commercial System includes a single longitudinal strain gauge at the midspan of three of the deck spans of the flyover. Fig. 11 shows a plot of longitudinal strain of a typical span measured at midspan. The recorded number of wire breaks of 1% of the tendon cross section over a 2-year period would result in a predicted strain change of $0.2\,\mu\varepsilon$, which cannot be detected with any confidence

given that there is a general background variation of approximately $40\,\mu\varepsilon$ in the readings, almost four times the predicted strain change expected for a loss of 20% of the prestressing wires. A large, unexplained shift in strain of approximately $100\,\mu\varepsilon$ in the concrete deck was detected during April and May 2011 (Fig. 11). A number of the other strain gauges, displacement transducers, and inclinometers also displayed a significant change at the same time, for which there does not appear to be an obvious physical explanation. This suggests that it is probably not a problem with any individual sensors; however, without further data from an independent monitoring system there is no way of verifying the cause. Unfortunately, the Research System was not functioning during this time and therefore no alternative data are available. However, even if this unexplained jump was not present, it would still not be possible to distinguish any small strain changes caused by prestress loss from the noise present in the data.

The background noise in the strain data readings means it is not possible to use measurements of decreasing strain on the cross section to validate the results obtained from the AE system. There is therefore no way of knowing whether the number of wire breaks detected by the system is correct. Because the Commercial System was not in place during the construction of the Hammersmith Flyover, it cannot provide absolute values for strain or number of broken wires. It instead only measures the changes in those values since the sensors were installed. It is therefore very difficult to determine the true state of the baseline for the condition model, which had to be determined by intrusive inspection. If such a system had been installed during the construction of the bridge, then, in principle, it would have been possible to establish acceptable thresholds for the number of wire breaks. Instead, the system can only be used to draw attention to the areas of the bridge experiencing the highest rates of deterioration.

TfL undertook extensive intrusive inspections and investigations to determine a benchmark condition of the posttensioning system as a baseline from which to build deterioration models of the structure incorporating the output from the acoustic monitoring systems (K. Duguid, personal communication, 2013).

Interpretation of Monitoring Data: Bearing Fixity Performance

The analysis in the previous section has shown that prestress losses resulting from breakages of up to 20% of the gross cross section of
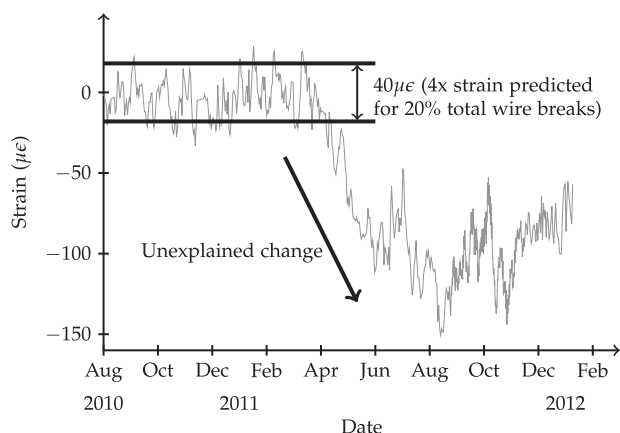
wires do not cause any measureable changes to the strains and displacements in the bridge superstructure. However, the installed sensors may be able to provide information about the state of the roller bearings supporting the bridge piers. Preliminary analyses are presented in Webb and Middleton (2013), but a more complete discussion follows here.

Piers: Axial Strains

Each pier has gauges measuring vertical strain on the concrete surfaces of both the eastern and western pier walls (Fig. 5). These should allow the combined effect of both axial and bending strains to be observed. If the roller bearings function correctly and allow unrestrained longitudinal movement of the pier bases, the piers should rotate rather than bend. Consequently, there should only be variations in axial strains caused by temperature and traffic live loading. Therefore, the strain gauges on the eastern and western sides of each pier should give similar readings. The monitoring system records temperatures in a variety of locations, allowing the strains due to temperature to be calculated. Temperature data from the bridge deck show a yearly range of approximately 25°C. In addition, there is a daily variation. In the top surface of the bridge deck, the daily range was found to be 10°C, whereas sensors in other locations gave a smaller daily range of approximately 2°C. The larger range of temperature observed in the top slab will be due in part to insolation and the black surfacing absorbing and radiating heat more rapidly than other surfaces.

Assuming a thermal expansion coefficient, α, for the concrete of $12 \times 10^{-6}/°C$, a yearly strain range of $25 \times 12 = 300\,\mu\varepsilon$ would be expected, with a daily cyclic variation of between $2 \times 12 = 24\,\mu\varepsilon$ and $10 \times 12 = 120\,\mu\varepsilon$.

Fig. 12 shows a plot of the vertical strain measured on the walls of a typical pier. The expected cyclic nature of the yearly variation due to temperature is not visible in the readings. Instead, there appears to be a long-term trend of increasing compressive strain. Because there is only a single strain sensor in each measuring location, it is impossible to verify whether the readings are valid or whether they are caused by drift of the monitoring system.

Piers: Longitudinal Displacement at the Bearing Level

Both the Commercial and Research monitoring systems measure longitudinal displacements at the bases of the piers (Fig. 5). The actual overall loading applied to the bridge at any time is not quantifiable because the live load cannot be measured. However, the
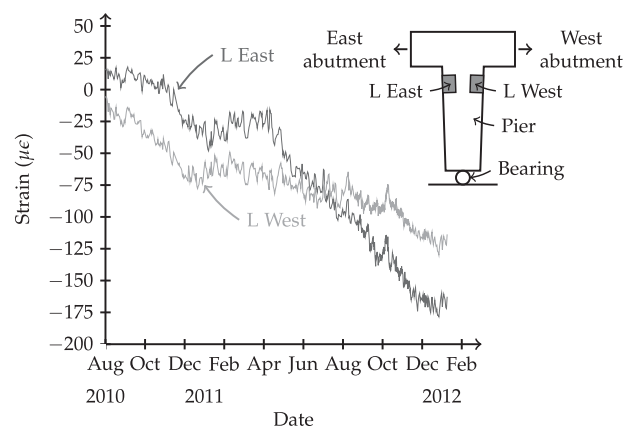

Fig. 11. Measured longitudinal strain at midspan of a typical span (2010–2012)

Fig. 12. Measured vertical strain in pier L (2010–2012)

relative effects of different loading types can be modeled. Using a simple plane frame beam model of the eastern half of the flyover created in the LUSAS finite-element package, the values of the parameters expected to be measured by each sensor can be predicted. A number of different load cases (Table 1) were assumed in the modeling exercise.
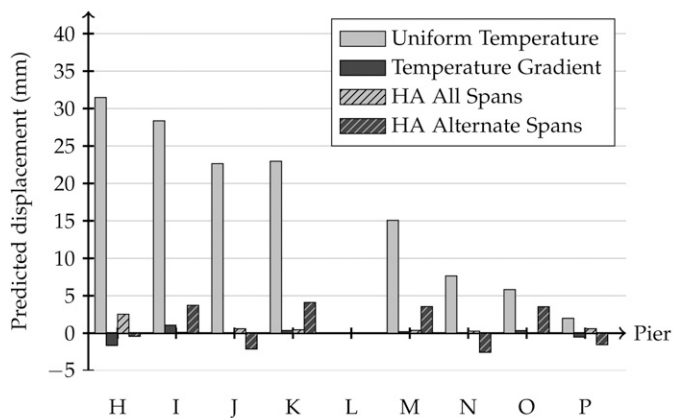
Fig. 13(a) shows the predicted displacements for each pier for each of these load cases when all bearings are functioning correctly

Table 1. Load Cases Used in LUSAS Analysis

Load case	Description
1	Uniform 10°C temperature increase, applied to all elements of the structure
2	Vertical temperature gradient of 3°C/m applied through the depth of the deck elements
3a	Standard HA traffic live loading model (from BD37/01 Appendix A, Section 6.2; Highways Agency 2002); a uniform and knife-edge load was applied to every span in the model to simulate the largest traffic load likely to be applied
3b	The standard HA traffic live loading was applied to alternate spans to allow the effects of uneven traffic distributions to be modeled
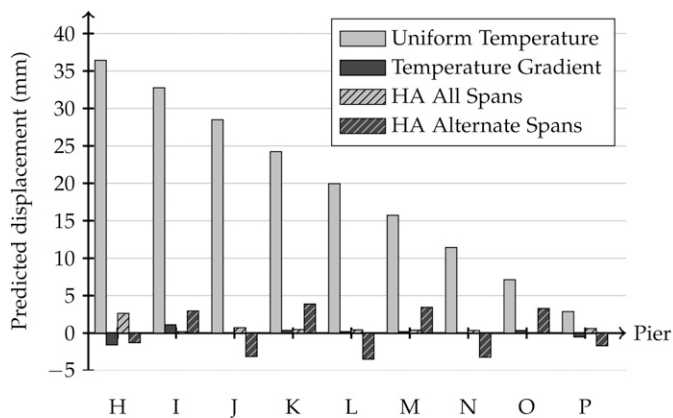
(a) All bearings free

(b) One bearing pinned (at pier L), others free

Fig. 13. Predicted displacements for various load cases: (a) all bearings free; (b) one bearing pinned (at pier L), others free (HA loading is defined in Table 1)

allowing unrestrained longitudinal movement, as symbolized by the design fixity shown in Fig. 4. Displacement at the bases of the piers is predominantly caused by uniform temperature increases, with the other loading scenarios considered having a much smaller effect. This suggests that plotting displacement of the base of the piers against temperature should show a good correlation if the bearings are functioning correctly.

Subsequently, the analyses were repeated with the support at one pier (pier L) assumed fixed to prevent any longitudinal displacement, simulating a corroded and jammed bearing. In Fig. 13(b), it can be seen that, with the exception of pier L, the predicted displacements of the piers are very similar to those shown in Fig. 13(a) (the undamaged scenario). Repeating the aforementioned analysis with any other pier assumed fixed results in a similar outcome. This means that deterioration of one of the bridge's bearings is not expected to significantly alter the displacements measured at the other piers. This should make it possible to determine the state of any bearing if the correlation between temperature and movement is no longer present.

Fig. 14 shows plots of both predicted and measured values of horizontal displacement against temperature for the bases of the piers in the eastern half of the bridge. The predicted displacements are based on the assumption that all bearings were working and unrestrained. Because the zero offset for pier displacement is arbitrary, the plots have been shifted vertically such that they all pass through the origin. This allows for easy comparison of the gradients.

For each pier, there appears to be a good linear relationship, suggesting that pier displacements are caused predominantly by temperature changes, as expected. A hysteresis effect can be seen, caused by the thermal mass of the bridge taking time to react to temperature changes. The actual measured displacements of seven of the piers (H, I, J, K, L, M and O) compare very well with the predictions, whereas piers N and P do not. Although these two piers move with temperature variations, they do not move to the same extent as would be expected from the modeling predictions. This implies that the bearings for these piers behave as if partially restrained and do not allow completely free longitudinal movement. No access to pier P was available to the authors; however, inspection of the bearings at pier N revealed the cause at that location. In each bearing pit, in addition to the bearings supporting the pier, there are also four steel plinths designed to prevent catastrophic damage occurring if any of the bearings were to fail by only allowing the pier to drop by a few millimeters. During construction, metal shim plates were inserted between the top of the plinths and the base of each pier to maintain a gap of approximately 13 mm (Rawlinson and Stott
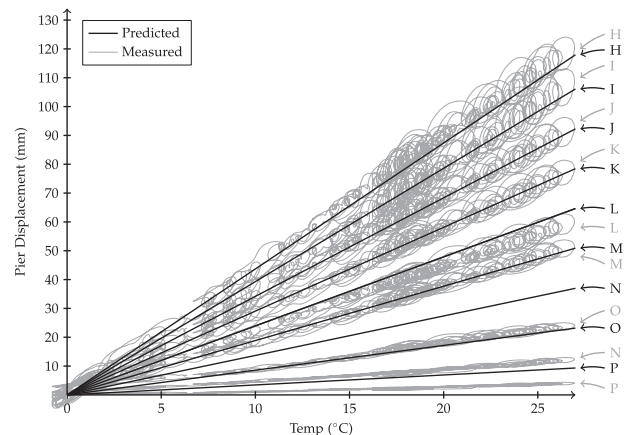

Fig. 14. Predicted and measured longitudinal displacement versus temperature plots for piers H to P

Concrete spalling   Corroded metal shims

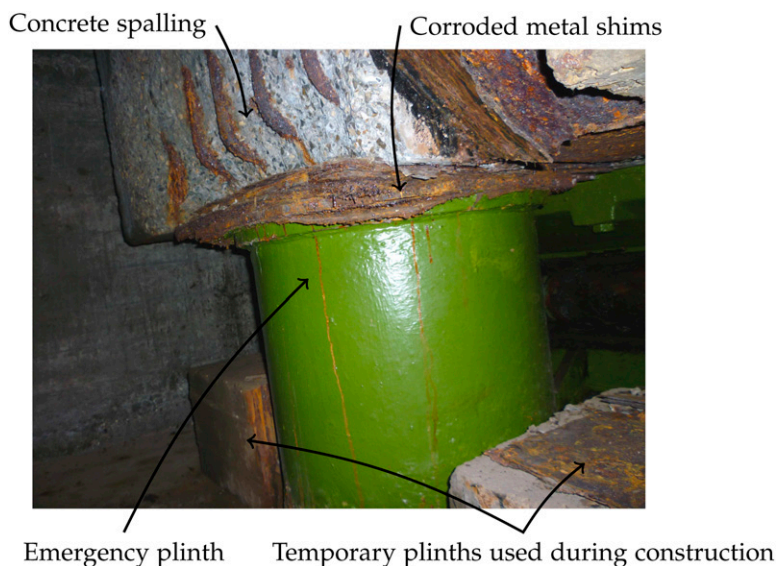Emergency plinth   Temporary plinths used during construction

Fig. 15. Base of pier N showing metal shims (image by authors, taken February 8, 2011)

1962). Fig. 15 shows pier N in 2012 with the shims in place but they have corroded over the last 50 years and become wedged between the pier and the plinth, restricting horizontal movement of the pier.

Discussion

This paper has described some of the interpretation of monitoring data on Hammersmith Flyover in London. This critical piece of aging infrastructure is a pertinent example of where SHM systems can provide some value in terms of understanding the performance of the structure to assist in its management (e.g., the effects of temperature and performance of the roller bearings). Having said this, the engineering information that can be gleaned from the collected data requires considerable postprocessing and interpretation by the structural engineer. Simply having a SHM system installed does not mean that valuable engineering information exists, merely that the data collected may have the potential to be converted into useful information with the appropriate filtering and analysis. It is important for engineers to carefully consider what parameters to measure, where to measure, and how to transform the data obtained into information that assists decision making. They must also consider whether the magnitude of the effect being monitored is large enough to be reliably detected and not masked by noise from other sources.

Summary

In summary, the monitoring sensors that provided useful data (once analyzed and interpreted) were AE for detecting wire breaks, LPDT readings to measure pier-bearing horizontal displacement, and temperature readings. Some specific summary points from the results of the monitoring project and the subsequent analyses are as follows:

1. Successful deployment of a robust and reliable SHM system is a challenging exercise; for such a system to be useful, consideration also needs to be given to how the collected data are to be interpreted;
2. The increasing rate of suspected wire breaks from the AE data provided guidance to the investigators as to which areas

warranted further visual inspection; this process led to the discovery of severe corrosion and subsequent closure of the flyover; SHM systems such as these will not replace visual inspection for corrosion but they will help target the inspections;
3. Attempting to use measurement of longitudinal strain in the bridge deck to detect changes caused by even a large number of wire breaks is not feasible because noise in the data due to live load effects make it impossible to assess whether prestress losses have occurred or not; the simple hypothetical analysis presented shows that the strain readings that a monitoring system would need to measure to detect realistic losses of prestress are very small and beyond the practical capability of any currently available measurement system; and
4. Measurements from both the Commercial and Research Systems have indicated that two of the flyover's pier bearings are partially restrained, rather than freely allowing longitudinal movement as had been intended by the designers; this was verified in the case of one pier (pier N) by visual inspection.

Acknowledgments

Notation

The following symbols are used in this paper:

A_c = cross-sectional area of concrete;

A_s = total cross-sectional area of prestressing steel wires;

E_c = Young's modulus of concrete;

E_s = Young's modulus of steel;

F_c = total force carried by concrete (compression positive);

$F_{c,\text{new}}$ = total force carried by concrete after wire break (compression positive);

F_i = total initial prestressing force (for all wires);

F_s = total force carried by steel wires (compression positive);

$F_{s,\text{new}}$ = total force carried by steel wires after wire break (compression positive);

H, I, J, K, etc. = the pier identification letters for the flyover used in this paper [they are the same as those adopted in the original bridge design (Fig. 1 in Rawlinson and Stott 1962)];

$k_{s,\text{eff}}$ = effective axial stiffness of all steel wires;

k_1 = axial stiffness of undamaged steel wires;

k_2 = axial stiffness of steel over effective break length;

l = hypothetical beam length;

l_b = effective wire break length;

x = length change of beam to restore equilibrium;

y = observed shortening of ends of broken wire;

α = coefficient of thermal expansion;

ΔA_s = reduction in total steel cross-sectional area due to wire break;

Δl = change in length of hypothetical beam;

$\Delta \varepsilon_c$ = change in concrete strain due to wire break;

$\Delta \sigma_s$ = change in total stress in steel over effective break length;

$\Delta \sigma_w$ = change in stress in steel wire due to wire break;

$\mu \varepsilon$ = microstrain;

σ_{ci} = total initial concrete stress (compression positive) = F_i / A_c; and

σ_{si} = initial steel stress (compression positive) = $-F_i / A_s$.

References

Catbas, F. N., Ciloglu, S. K., Hasancebi, O., Grimmelsman, K., and Aktan, A. E. (2007). "Limitations in structural identification of large construction structures." *J. Struct. Eng.*, 10.1061/(ASCE)0733-9445(2007)133:8(1051), 1051–1066.

Chang, S. P., and Im, C. K. (2000). "Thermal behaviour of composite box-girder bridges." *Proc. Inst. Civ. Eng., Struct. Build.*, 140(2), 117–126.

Dwairi, H. M., Wagner, M. C., Kowalsky, M. J., and Zia, P. (2010). "Behavior of instrumented prestressed high performance concrete bridge girders." *Construct. Build. Mater.*, 24(11), 2294–2311.

Farrar, C. R., and Worden, K. (2007). "An introduction to structural health monitoring." *Philos. T. Roy. Soc. A*, 365(1851), 303–315.

Goulet, J.-A., Kripakaran, P., and Smith, I. F. C. (2010). "Multimodel structural performance monitoring." *J. Struct. Eng.*, 10.1061/(ASCE)ST.1943-541X.0000232, 1309–1318.

Hada, A., et al. (2011). "Condition monitoring system for railway structures in Hammersmith." *Proc., Ninth World Congress on Railway Research*, Société Nationale des Chemins de fer Français (SNCF), Paris.

Hedegaard, B. D., French, C. E. W., Shield, C. K., Stolarski, H. K., and Jilk, B. J. (2013). "Instrumentation and modeling of I-35W St. Anthony Falls Bridge." *J. Bridge Eng.*, 10.1061/(ASCE)BE.1943-5592.0000384, 476–485.

Highways Agency. (2002). "BD37/01 loads for highway bridges." *Design manual for roads and bridges*, ⟨http://www.dft.gov.uk/ha/standards/dmrb/vol1/section3/bd3701.pdf⟩ (Apr. 13, 2013).

Hoult, N. A., et al. (2010a). "Large-scale WSN installation for pervasive monitoring of civil infrastructure in London." *Proc., Fifth European Workshop on Structural Health Monitoring*, F. Casciati, and M. Giordano, eds., DEStech Publications, Lancaster, PA, 214–219.

Hoult, N. A., Fidler, P. R. A., Hill, P. G., and Middleton, C. R. (2010b). "Long-term wireless structural health monitoring of the Ferriby Road Bridge." *J. Bridge Eng.*, 10.1061/(ASCE)BE.1943-5592.0000049, 153–159.

Hoult, N. A., Fidler, P. R. A., Middleton, C. R., and Hill, P. G. (2008a). "Turning the Humber Bridge into a smart structure." *Proc., Fourth Int. IABMAS Conf.*, H.-M. Koh and D. Frangopol, eds., CRC Press, Leiden, Netherlands, 1402–1409.

Hoult, N. A., Fidler, P. R. A., Wassell, I. J., Hill, P. G., and Middleton, C. R. (2008b). "Wireless structural health monitoring at the Humber Bridge U.K." *Proc. Inst. Civ. Eng., Bridge Eng.*, 161(4), 189–195.

Kripakaran, P., and Smith, I. F. C. (2009). "Configuring and enhancing measurement systems for damage identification." *Adv. Eng. Inform.*, 23(4), 424–432.

Kurata, M., et al. (2013). "Internet-enabled wireless structural monitoring systems: Development and permanent deployment at the new Carquinez Suspension Bridge." *J. Struct. Eng.*, 10.1061/(ASCE)ST.1943-541X.0000609, 1688–1702.

Laory, I., Ali, N. B. H., Trinh, T. N., and Smith, I. F. C. (2012). "Measurement system configuration for damage identification of continuously monitored structures." *J. Bridge Eng.*, 10.1061/(ASCE)BE.1943-5592.0000386, 857–866.

Lynch, J. P. (2007). "An overview of wireless structural health monitoring for civil structures." *Philos. T. Roy. Soc. A*, 365(1851), 345–372.

Lynch, J. P., and Loh, K. J. (2006). "A summary review of wireless sensors and sensor networks for structural health monitoring." *Shock Vib*, 38(2), 91–128.

Lynch, J. P., Wang, Y., Loh, K. J., Yi, J.-H., and Yun, C.-B. (2006). "Performance monitoring of the Geumdang Bridge using a dense network of high-resolution wireless sensors." *Smart Mater. Struct.*, 15(6), 1561–1575.

Maser, K. (1988). "Sensors for infrastructure assessment." *J. Perform. Constr. Facil.*, 10.1061/(ASCE)0887-3828(1988)2:4(226), 226–241.

Minardo, A., Persichetti, G., Testa, G., Zeni, L., and Bernini, R. (2012). "Long term structural health monitoring by Brillouin fibre-optic sensing: A real case." *J. Geophys. Eng.*, 9(4), S64–S69.

Rawlinson, J., and Stott, P. F. (1962). "The Hammersmith Flyover." *Proc. Inst. Civ. Eng.*, 23(4), 565–600.

Shoukry, S. N., Riad, M. Y., and William, G. W. (2009). "Long term sensor-based monitoring of an LRFD designed steel girder bridge." *Eng. Struct.*, 31(12), 2954–2965.

Watson, J. (2010). "Watching brief." *Bridge Design and Eng.*, 60, 67.

Webb, G. T., and Middleton, C. R. (2013). "Structural health monitoring of the Hammersmith Flyover." *Proc., IABSE Conf. Rotterdam 2013 Assessment, Upgrading and Refurbishment of Infrastructures* (CD-ROM), IABSE, Zürich, Switzerland, 152–153.

Wong, K. Y. (2004). "Instrumentation and health monitoring of cable-supported bridges." *Struct. Contr. Health Monit.*, 11(2), 91–124.

Wroth, C. P. (1962). "The Hammersmith Flyover – Site measurements of prestressing losses and temperature movement." *Proc. Inst. Civ. Eng.*, 23(4), 601–624.